Data report: Site C0011 LWD resistivity–derived porosity[1]

Joanne Tudge,[2] Mike Lovell,[3] and Sarah Davies[3]

Chapter contents

[1]Tudge, J., Lovell, M., and Davies, S., 2013. Data report: Site C0011 LWD resistivity–derived porosity. *In* Saito, S., Underwood, M.B., Kubo, Y., and the Expedition 322 Scientists, *Proc. IODP,* 322: Tokyo (Integrated Ocean Drilling Program Management International, Inc.). doi:10.2204/iodp.proc.322.201.2013
[2]Department of Geoscience, University of Wisconsin-Madison, 1215 West Dayton Street, Madison WI 53706, USA.
jtudge@geology.wisc.edu
[3]Department of Geology, University of Leicester, University Road, Leicester LE1 7RH, United Kingdom.

Abstract

During Integrated Ocean Drilling Program (IODP) Expedition 322 for the Nankai Trough Seismogenic Zone Experiment project, no logging-while-drilling (LWD)–based porosity measurements were acquired at Site C0011. Here we calculate porosity from both the ring and bit resistivity measurements. Core-derived thermal conductivity coefficients are used to estimate constant thermal gradients and variable thermal gradients for the different lithologies encountered. Temperature profiles are then generated based on the calculated thermal gradients to estimate water resistivity. Using the temperature-corrected water resistivity in Archie's equation, porosity is calculated from the two LWD resistivity measurements. When compared to core-based porosity measurements, the ring resistivity–derived porosity, with a constant thermal gradient of 91.3°C/km, provides the more accurate estimate of porosity.

Introduction

In the absence of any density, neutron, or sonic data at Integrated Ocean Drilling Program (IODP) Site C0011, log-based porosity was calculated from the logging-while-drilling (LWD) resistivity data. Of the five available resistivity measurements (ring, bit, and three button), porosity was calculated from ring and bit resistivity. Bit and ring resistivity were chosen for comparison, as they provide two different resolutions. Bit resistivity measures directly behind the drill bit with a low vertical resolution (30–60 cm), whereas ring resistivity is a focused measurement with a vertical resolution of 5–8 cm (Schlumberger, 2007). The calculation of a bit resistivity–derived porosity at Site C0011 also ensures a consistent data set across the Nankai Trough Seismogenic Zone Experiment (NanTroSEIZE) drilling transect, as LWD bit resistivity porosity was calculated at IODP Sites C0001–C0006 (Kinoshita et al., 2008).

Archie porosity estimation

To estimate porosity from the LWD resistivity data, Archie's equation is used. Archie (1942) determined an empirical relationship between the porosity (ϕ) of a formation and the formation factor (FF):

doi:10.2204/iodp.proc.322.201.2013

$$FF = a/\phi^m, \quad (1)$$

where a is a constant and m reflects the pore geometry and interpore connections (known as the cementation exponent). Usually m and a are determined from core sample measurements.

The formation factor (FF), originally defined by Sundberg (1932), is the ratio of resistivity of a fully water-saturated rock (R_o) to the resistivity of the saturating fluid (R_w):

$$FF = R_o/R_w. \quad (2)$$

By combining Equations 1 and 2 to produce Equation 3, it is possible to relate the formation resistivity (R_o) to the porosity (ϕ):

$$R_o/R_w = a/\phi^m. \quad (3)$$

If the resistivity of the saturating fluid, cementation exponent, and constant a are known, then the porosity can be calculated from the measured LWD resistivity (Equation 4), as the LWD resistivity measures the resistivity of the fully saturated rock (R_o):

$$FF = (aR_w/R_o)^{1/m}. \quad (4)$$

The resistivity of the formation water, in this case dominantly seawater, changes with temperature. Shipley, Ogawa, Blum, et al. (1995) defined the relationship between the fluid resistivity (R_w) and borehole temperature as

$$R_w = 1/(2.8 + 0.1T), \quad (5)$$

where T is the temperature in degrees Celsius (Shipley, Ogawa, Blum, et al., 1995). In order to use the above equation, a downhole temperature profile must be estimated. Given the lack of any bottom-hole temperatures from the logging data, core data thermal conductivity measurements were used to estimate temperature gradients.

Temperature estimation

The thermal conductivity coefficient (k) can be measured directly from core samples (Blum, 1997) and relates to heat flow (q) across a steady-state temperature (T) difference over distance (x):

$$q = k(\Delta T/\Delta x). \quad (6)$$

The change in temperature over a set distance ($\Delta T/\Delta x$) is the thermal gradient and can be used to give an estimate of downhole temperature.

At Site C0011, no LWD temperature measurements were available, so core data were used to generate a temperature estimate. Surface heat flow in Hole C0011B was determined to be 89.5 mW/m², with a surface temperature of 1.7°C and an average thermal gradient of 93.1°C/km (Expedition 333 Scientists, 2012). Temperature gradients were calculated using core-based thermal conductivity coefficients from Holes C0011B and C0011D, obtained during IODP Expeditions 322 and 333, respectively (see the "Site C0011" chapter [Expedition 322 Scientists, 2010]; Expedition 333 Scientists, 2012) (Fig. F1). Average thermal conductivities were determined for the entire data set, for each of the lithologic units, and for the two main lithologies encountered (Table T1).

Using the core thermal conductivity measurements, four temperature profiles were generated (Fig. F1). Two were generated from constant temperature gradients: Temp C1 was based on the constant thermal gradient of 91.3°C/km reported during Expedition 333 (Expedition 333 Scientists, 2012) and Temp C2 was based on a thermal gradient of 80.7°C/km, which was calculated from the average thermal conductivity of both Hole C0011B and C0011D core data. Additionally, two variable temperature profiles were calculated: Temp V1 was based on the thermal gradient of each lithologic unit and Temp V2 was based on the average thermal gradient of the dominant lithology (Table T1). The dominant lithology was chosen on the core-based lithologic units converted to meters below seafloor based on the log depth measurement (LWD depth below seafloor). Each temperature profile yields a different bottom-hole temperature (Table T2), but none can be verified in the absence of a bottom-hole temperature measurement. However, each temperature profile can be used to calculate a temperature-corrected R_w, and the subsequent porosity profiles can be compared to core porosity to determine the most accurate calculation.

Porosity calculations

Using the previously discussed Archie relationship between porosity (ϕ) and measured LWD resistivity (R_o) and the temperature-corrected fluid resistivity (R_w) it is possible to estimate a complete porosity profile. As determined from previous work in the

Nankai Trough area and previous NanTroSEIZE expeditions (Kinoshita et al., 2008), m = 2.4 and a = 1. Both bit and ring resistivity were used to calculate two separate porosity profiles, for each temperature-corrected fluid resistivity.

Results

The calculated porosity profiles were compared to the core porosity (Fig. F2). Because of the poor quality of the recovered core (see the "Site C0011" chapter [Expedition 322 Scientists, 2010]), the core-based porosity measurements exhibit a lot of scatter. However, the general trend and concentration of data points can be matched to the LWD resistivity porosities.

For each of the constant and variable thermal gradient results, bit resistivity porosity exhibits a very similar trend to ring resistivity porosity but always at slightly lower values and with less scatter. Considering the difference in vertical resolution of the bit and ring resistivity measurements, the smooth nature of the bit resistivity porosity is most likely caused by the large volume of investigation. Because ring resistivity offers a more focused and better vertical resolution than bit resistivity, the ring resistivity–derived porosity is taken to be the more accurate and reliable of the two resistivity porosity estimates.

In relation to the variation between the porosity calculated from the variable thermal gradients and that calculated from the constant thermal gradients, there is very little difference, most likely due to the very similar data ranges seen in the core data. However, the constant thermal gradient of 91.3°C/km (Temp C1) gives a slightly improved fit to the core data, particularly through the upper section of lithologic Unit I (Fig. F2).

Overall, the most accurate LWD resistivity–based porosity estimate is calculated from ring resistivity, using the fluid resistivity corrected for temperature based on the constant temperature gradient recorded during Expedition 333. Therefore, it is suggested that for further analysis this porosity estimate should be used.

Acknowledgments

Data for this paper were provided by the Integrated Ocean Drilling Program (IODP). J. Tudge sailed as a logging scientist, funded by the National Environment Research Council (NERC), and was subsequently supported by NERC (NE/H013636/1).

References

Archie, G.E., 1942. The electrical resistivity log as an aid in determining some reservoir characteristics. *Trans. Am. Inst. Min., Metall. Pet. Eng.,* 146:54–62.

Blum, P., 1997. Physical properties handbook: a guide to the shipboard measurement of physical properties of deep-sea cores. *ODP Tech. Note,* 26. **doi:10.2973/odp.tn.26.1997**

Expedition 322 Scientists, 2010. Site C0011. *In* Saito, S., Underwood, M.B., Kubo, Y., and the Expedition 322 Scientists, *Proc. IODP,* 322: Tokyo (Integrated Ocean Drilling Program Management International, Inc.). **doi:10.2204/iodp.proc.322.103.2010**

Expedition 333 Scientists, 2012. Site C0011. *In* Henry, P., Kanamatsu, T., Moe, K., and the Expedition 333 Scientists, *Proc. IODP,* 333: Tokyo (Integrated Ocean Drilling Program Management International, Inc.). **doi:10.2204/iodp.proc.333.104.2012**

Kinoshita, M., Tobin, H., Moe, K.T., and the Expedition 314 Scientists, 2008. NanTroSEIZE Stage 1A: NanTroSEIZE LWD transect. *IODP Prel. Rept.,* 314. **doi:10.2204/iodp.pr.314.2008**

Schlumberger, 2007. *geoVISION: Resistivity Imaging for Productive Drilling:* Houston (Schlumberger). **http://www.slb.com/~/media/Files/drilling/brochures/lwd/vision/geovision.pdf**

Shipley, T.H., Ogawa, Y., Blum, P., et al., 1995. *Proc. ODP, Init. Repts.,* 156: College Station, TX (Ocean Drilling Program). **doi:10.2973/odp.proc.ir.156.1995**

Sundberg, K., 1932. Effect of impregnating waters on electrical conductivity of soils and rocks. *Trans. Am. Inst. Min. Metall. Pet. Eng.,* 79:367–391.

Initial receipt: 1 November 2010
Acceptance: 21 March 2013
Publication: 22 May 2013
MS 322-201

Figure F1. Temperature gradient calculated from the core-based thermal conductivities, showing both a consistent gradient and one with variations for the dominant lithology, Site C0011.

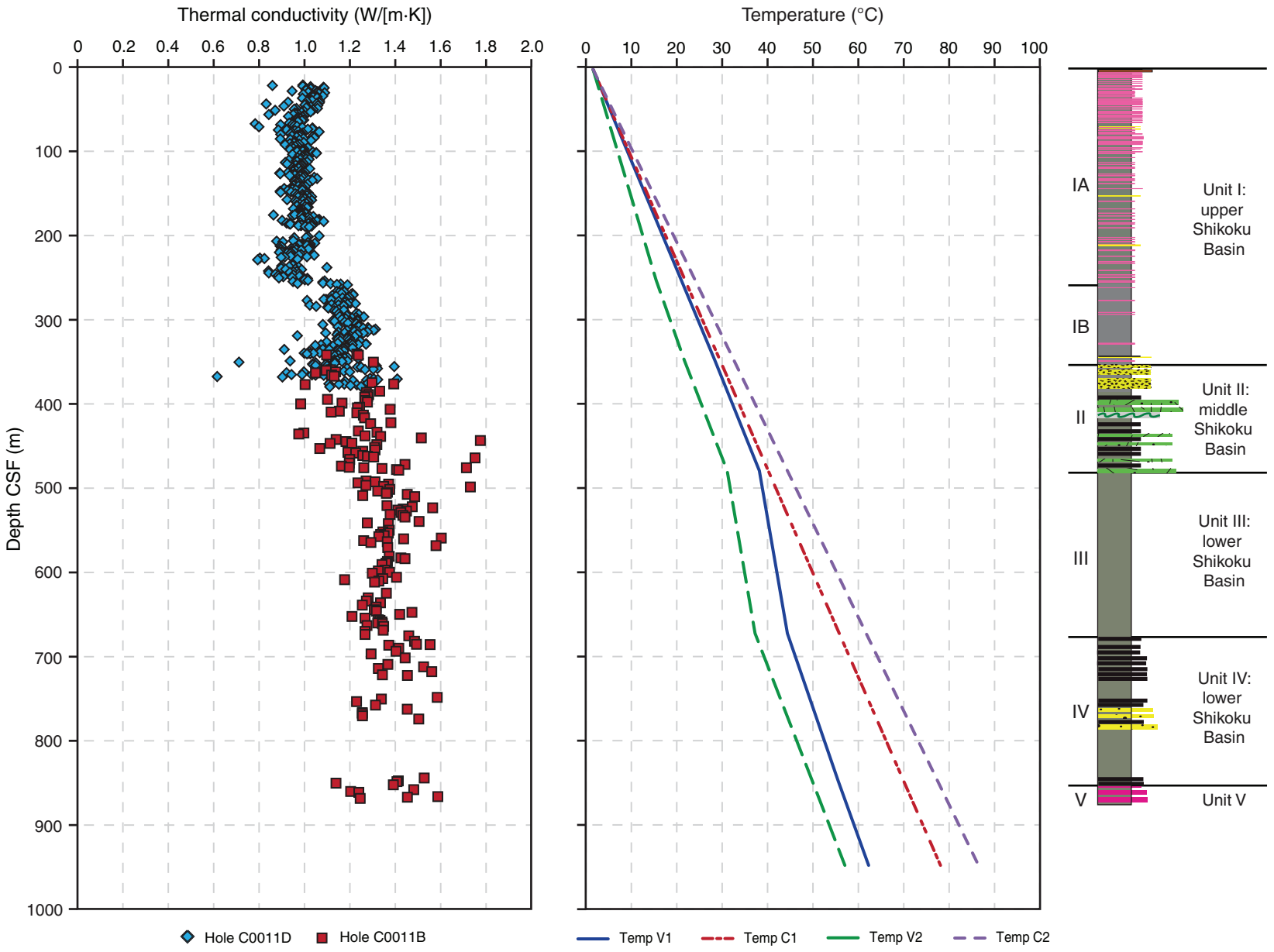

Figure F2. Bit and ring resistivity profiles compared to core porosity measurements using R_w calculated from Temp C1, Temp C2, Temp V1, and Temp V2 at Site C0011. All exhibit a good match between calculated porosity and core porosity, considering the scatter of the core data.

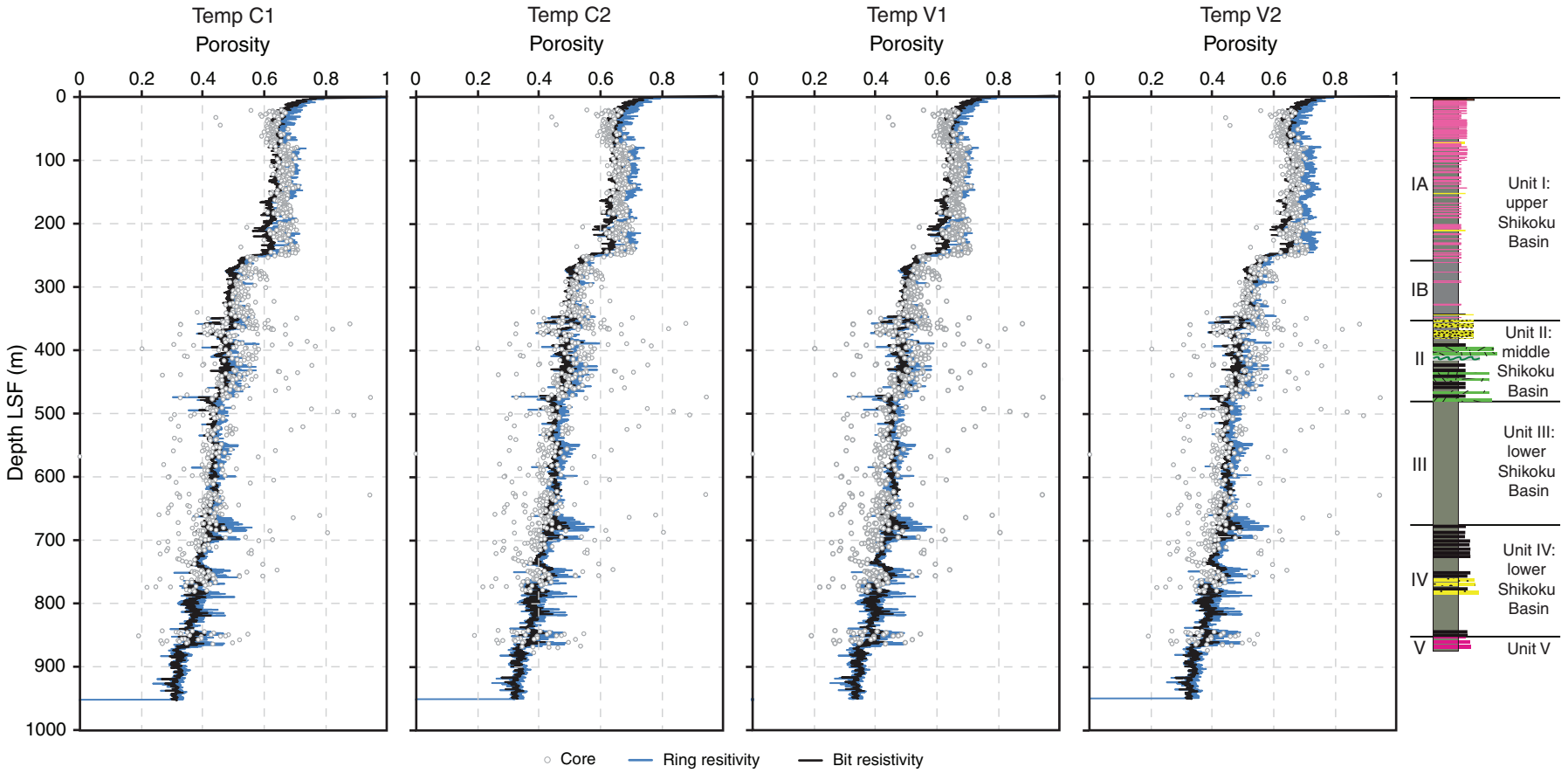

Table T1. Thermal conductivity coefficients from core data and the subsequent calculated thermal gradients for bulk lithologies and lithologic unit, Site C0011.

		Depth range CSF (m)	Average coefficient of thermal conductivity	Thermal gradient (°C/km)	Dominant lithology
Lithology	Mudstone		1.37	65.3	
	Sandstone		1.25	71.6	
Lithologic unit	IA	0.00–251.52	0.97	91.57	Hemipelagic mudstone
	IB	251.52–347.82	1.16	77.32	Hemipelagic mudstone
	II	347.82–479.50	1.2	74.49	Volcanic sandstone
	III	479.50–673.90	1.36	65.68	Hemipelagic mudstone
	IV	673.90–849.90	1.41	63.52	Sandstone/Siltstone turbidites
	V	849.90–951.00	1.34	66.64	Volcaniclastic turbidites

Table T2. Estimated bottom-hole temperatures for calculated temperature profiles, Site C0011.

Temperature profile	Thermal gradient (°C/km)	Bottom-hole temperature (°C)
Temp C1	91.3	86.82
Temp C2	80.7	78.41
Temp V1	Per lithologic unit	62.5
Temp V2	Per dominant lithology	57.3